PATH LOSS PREDICTION FOR LOW-RISE BUILDINGS WITH IMAGE CLASSIFICATION ON 2-D AERIAL PHOTOGRAPHS

S. Phaiboon

Electrical Engineering Department
Faculty of Engineering
Mahidol University
Salaya, Nakhon Pathom 73170, Thailand

P. Phokharatkul

Computer Engineering Department
Faculty of Engineering
Mahidol University
Salaya, Nakhon Pathom 73170, Thailand

Abstract—This paper presents a radio wave propagation prediction method for low-rise buildings using 2-D aerial images taken from the actual areas. The prediction procedure was done in three steps. Firstly, the images were classified in order to identify the objects by Color Temperature Properties with Maximum Likelihood Algorithm (CTP_MLA). The objects in the images consist of buildings, trees, roads, water and plain. These objects influence wave propagation highly. The MLA classification is a common supervised image segmentation technique in remote sensing domain. However it still needs human editing in case of classification errors. Secondly, the appropriate path loss models were selected to predict path loss. The original Xia path loss model was modified to include the effects of airy buildings and vegetation around the buildings. Finally, preliminary tests provide a better solution compared with measured path losses with the root mean square error (RMSE) and maximum relative error (MRE) of 3.47 and 0.31, respectively. Therefore, the positions for micro-cell base stations could be designed on a 2-D aerial map.

_____

Corresponding author: S. Phaiboon (egspb@mahidol.ac.th).

1. INTRODUCTION

Cellular mobile network planning is necessary to provide highly efficient services. Thus, we require a tool which is easy to use in planning the cellular network with high accuracy. There are many tools or models for cellular network planning such as empirical models with 2-D databases and semi-deterministic models with 2.5D databases, including deterministic models with 3-D databases. The empirical models are easy to use with fast calculations but sometime they have accuracy problems in different areas, while the semi-deterministic model such as the Walfisch-Ikegami model provides high accuracy prediction and requires a ground survey of the environment; in addition, the deterministic models provide high accuracy in path loss prediction. However, they need details of the environment database and take a lot of time for calculating.

For semi-deterministic models, there are previous studies as follows. Xia et al. [1, 2] proposed path loss formulas for micro-cells in low-rise and high-rise building environments. Additionally, COST 231 Walfisch-Ikegami model [3, 4] is also a popular prediction tool for micro cell environments. However, they need environment database details such as building height, street width etc. Oda et al. [5] found the effect of the equivalent ground plane due to traffic on the road in a LOS path loss model. Jiang et al. [6] proposed a simple analytical path loss model using rectangular shaped blocks with equal height. Additionally, Masui et al. [7] proposed upper and lower bounds LOS path loss models at frequencies of 3.35, 8.45, and 15.75 GHz. In forest environments, Durgin et al. presented measurement and empirical models for path loss in and around homes and trees at a frequency of 5.85 GHz [8]. They introduced 10–16 dB of tree loss in excess of free space path loss. Karlsson et al. also introduced 10 dB of the tree loss at frequencies of 3 and 5 GHz [9]. Torrico et al. [10, 11] proposed calculated tree-specific attenuation (dB/m) in a frequency range of 0.8 to 2.0 GHz. Meng et al. [12] presented frequency-domain characterization of short range tropical foliage channels. They presented first Fresnel zone region of tree environments.

In the propagation environments, there are several categories of environments such as buildings, trees, roads, water and homes. Practically, it is difficult to survey these categories of the environments especially in urban environments. Although prediction of path loss based on aerial photographs has been performed for outdoor communications at a frequency of 1.8 MHz [13], processing either raster or vector formats on the map were not provided in details and took a lot of time.

To solve these problems, this paper proposes a new cellular planning tool using image classification of aerial images. The images were classified by the CTP_MLA to identify the objects in the areas of interest, such as buildings, roads, trees, plains and water. Then, a appropriate path loss model for the individual environment category was selected to predict path loss on the available maps.

In this paper, we present the image classification in Section 2. Path loss prediction is presented in Section 3. Measurement procedure and sites are presented in Section 4. The resulting comparisons are presented in Section 5. Finally, the conclusion is drawn in Section 6.

2. IMAGE CLASSIFICATIONS

Objects in the aerial image are identified using an image classification. However, the image classification is not entirely automated. The division into zones has been supervised and corrected by human intervention. There are many algorithms for the image classification such as watershed algorithm, Fuzzy C-means algorithm and color-texture fusion with maximum likelihood algorithm, etc. This research employed the CTP_MLA. It uses a statistical analysis to provide the least error as shown in our previous research [14]. Maximum Likelihood (ML) was proposed by Perkins in 1999 [15]. This approach uses Baye's theorem to compute the maximum likelihood decision rules and multivariate normal class models. Let the classes of an aerial image scene be represented by ω_i and the total classes be equal to M. After that, the classes or categories are determined, which a pixel at location x belongs to. The conditional probability $p(\omega_i|x)$ is used to consider the likelihood value that correct the class ω_i for a pixel at position x. The performance of classification is to $x \in \omega_i$ if $p(\omega_i|x) > p(\omega_j|x)$ for all $j \neq i$, or the pixel at x belongs to the class ω_i if $p(\omega_i|x)$ has the largest value. In spite of the simplicity of this decision rule these posterior probabilities are unknown. Thus, training can be used to instead estimate the class-conditional probability density $p(\omega_i|x)$, which describes the chance of finding a feature vector from class ω_i at the spectral position x. The probability $p(\omega_i|x)$ gives the likelihood that the corrected class is ω_i for a pixel at position x. The desired $p(\omega_i|x)$ and available $p(\omega_i|x)$ are related by Baye's theorem as in Equation (1),

$$p(\omega_i|x) = \frac{p(x|\omega_i)p(\omega_i)}{p(x)} \tag{1}$$

where, $p(x|\omega_i)$ is the chance of finding a feature vector from class ω_i at the spectral position x; $p(\omega_i)$ is the prior (a priori) probability of class ω_i; $p(x)$ is the probability of finding any class at position x.

Using Baye's theorem the value of $p(x|\omega_i)$ can be obtained, so classification can be performed using

$$x \in \omega_i \text{ if } p(\omega_i|x) > p(\omega_j|x) \text{ for all } j \neq i \tag{2}$$

To test the above method, two aerial images were taken. The results of image classification of a village and dormitory buildings are shown in Figures 1 and 2 respectively. The aerial images are classified into 5 categories as follows, buildings (black), roads (red), forests (green), plain (light green) and water (blue). It can be seen that building errors in Figure 1 occur from green roof errors as shown in Figure 1(b). It
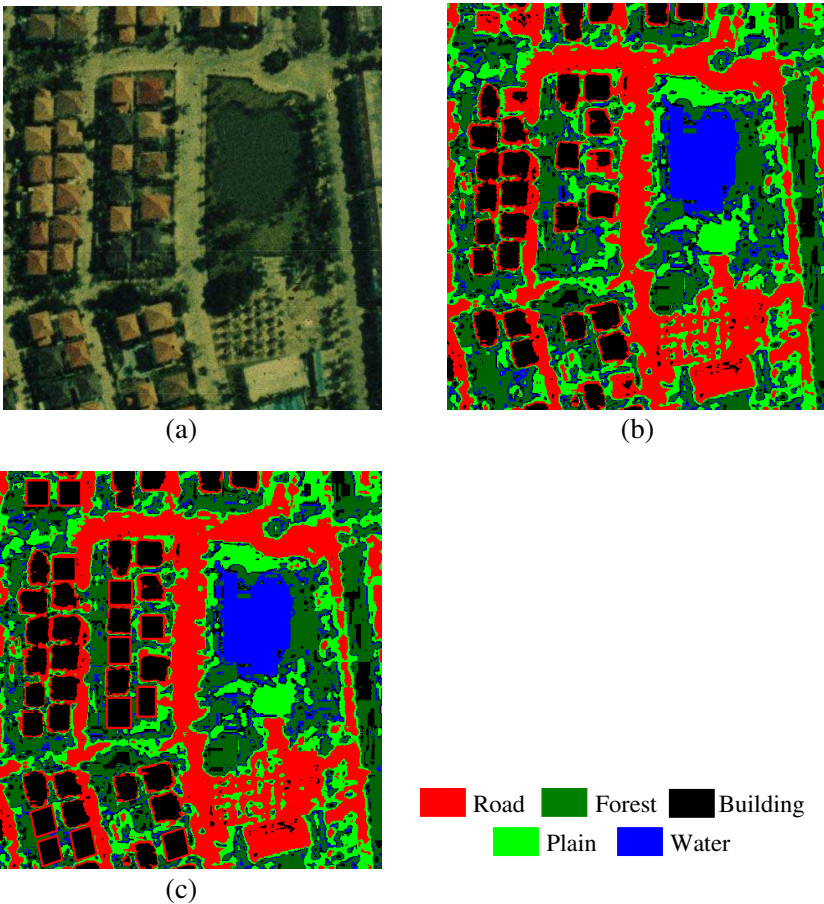

Figure 1. Image classification of a village: (a) Original image, (b) classified image, and (c) after editing.

is difficult for the training to separate them from trees. Additionally there are water errors in some tree areas because of green reflection in the water. We corrected the image classification errors by manually color editing as shown in Figure 1(c).

The second place is Namtong Sikharai dormitory in Mahidol University, Salaya Campus. After image classification, there are two errors between plain and water as shown in Figure 2(b) but their influences on wave propagation are not significant. However, manual color editing for vegetation is still needed. This is because the aerial image was taken in 2006 but the measurement was performed on March 2009. The vegetation was in small size so it was not classified. The complete editing and a side view photo of the area are shown in Figures 2(c) and 2(d) respectively.
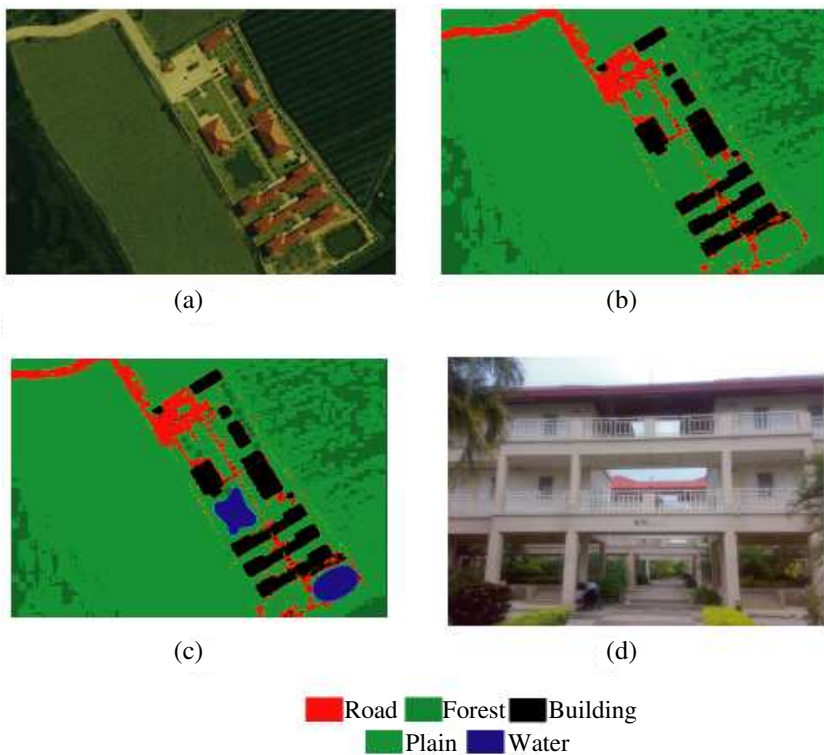

Figure 2. Image classification of dormitory: (a) Original image, (b) classified image, (c) after editing, and (d) a side view photo.

3. PATH LOSS PREDICTION

When waves propagate in urban or sub-urban environments, there are various propagation effects such as diffraction over rooftops and around building corners, scattering on buildings, penetration through vegetation, etc. In the case of an airy building which has no walls, the dominant wave does not diffract over the rooftops but it diffracts at the edge of the railing. Therefore, the radio network planning has to consider the above phenomenon. The path loss models are then divided into 3 subdivision areas: (i) Regular building area which composes of buildings with walls, (ii) Airy building area which composes of buildings without walls, and (iii) Vegetation area.

3.1. Regular Building Area

The original Xia model for low-rise environments with one-five story buildings was applied to predict path loss because it needed 2D maps of buildings for calculation. There are three routes for prediction namely, staircase, transverse and lateral routes as shown in Figure 3. A transmitter (Tx) was located on street in the middle of a building block. The original Xia path loss formulas [1] were written as

Staircase route:

$$
\begin{aligned}
P_L(d) \ = \ & [137.61 + 35.16 \log f_G] \\
& -[12.48 + 4.16 \log f_G] \mathrm{sgn}(\Delta h) \log(1 + |\Delta h|) \\
& +[39.46 - 4.13 \mathrm{sgn}(\Delta h) \log(1 + |\Delta h|)] \log d
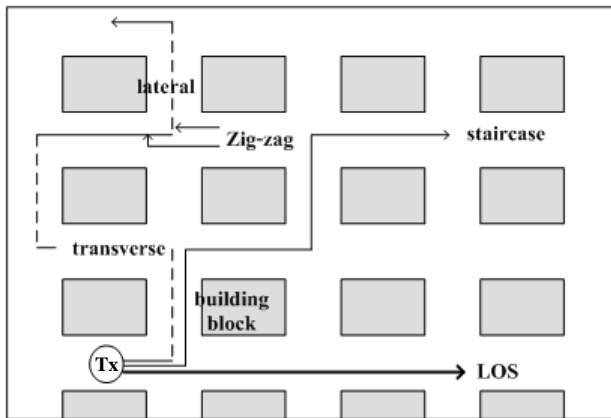\end{aligned}
\tag{3}
$$

Figure 3. Geometry of Xia model.

Transverse route:

$$
\begin{aligned}
P_L(d) = \ & [139.01 + 42.59 \log f_G] \\
& -[14.97 + 4.99 \log f_G]\mathrm{sgn}(\Delta h) \log(1 + |\Delta h|) \\
& +[40.67 - 4.57\mathrm{sgn}(\Delta h) \log(1 + |\Delta h|)] \log d \qquad (4)
\end{aligned}
$$

Lateral route:

$$
\begin{aligned}
P_L(d) = \ & [127.39 + 31.63 \log f_G] \\
& -[13.05 + 4.35 \log f_G]\mathrm{sgn}(\Delta h) \log(1 + |\Delta h|) \\
& +[29.18 - 6.70\mathrm{sgn}(\Delta h) \log(1 + |\Delta h|)] \log d \qquad (5)
\end{aligned}
$$

All non-LOS routes:

$$
\begin{aligned}
P_L(d) = \ & [139.01 + 42.59 \log f_G] \\
& -[14.97 + 4.99 \log f_G]\mathrm{sgn}(\Delta h) \log(1 + |\Delta h|) \\
& +[40.67 - 4.57\mathrm{sgn}(\Delta h) \log(1 + |\Delta h|)] \log d \\
& +20 \log(\Delta h_m/7.8) + 10 \log(20/d_h) \qquad (6)
\end{aligned}
$$

where

d is the mobile distance from transmitter (m). $[0.05 < d < 3]$,

f_G is the frequency (GHz). $[0.9 < f_G < 2]$,

Δh is the relative height of transmitter to average building height (m). $[-8 < \Delta h < 6]$,

Δh_m is the height of the last building relative to the mobile (m),

d_h is the distance of mobile from the last rooftop (m),

h_b is the transmitting antenna height from ground level (m),

h_m is the mobile antenna height from ground level (m) and

λ is the wavelength (m).

3.2. Airy Building Area

In the case of airy buildings which have no walls, the principle wave does not diffract at the roof edge but propagates through the building and diffracts at the edge of the railing as shown in Figure 4. This is because the vertical length of railings is larger than the wavelength. Equation (6) is also applied, but the average building height of rooftop is modified by

$$
\begin{aligned}
h_{BD(airy)} &= \sum_{i=1}^{n-1} H_i + h_r & \text{if } h_b < h_{BD} \\
&= h_{BD} & \text{if } h_b \geq h_{BD} \qquad (7)
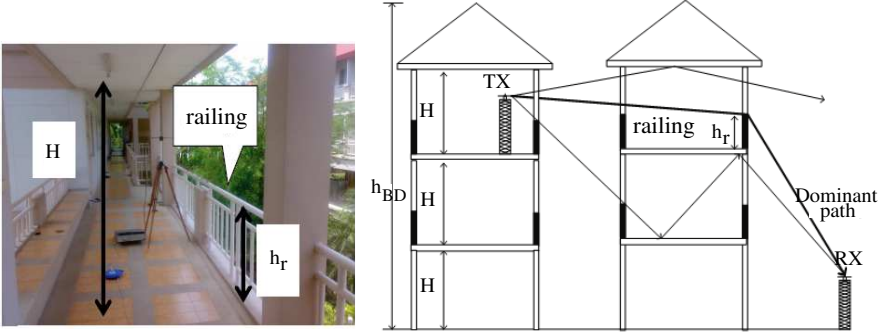\end{aligned}
$$

where

Figure 4. Geometry of airy building model.

H_i is the ceiling height of ith floor (m),

n is the floor's number which the dominant path propagates through the airy building,

h_r is the railing height (m) and

h_{BD} is the building height of the rooftop (m).

If the buildings between the transmitter and the receiver are both the airy and regular buildings, the average building height must be calculated. It is an average between the height of h_{BD} (airy buildings) in (7) and the height of rooftop of h_{BD} (regular buildings). This average value is used in (6).

3.3. Vegetation Area

When the wave propagation passes through tree area as shown in Figure 5(a), it is attenuated following the Torrico model [10, 11]. The specific attenuation for an ensemble of thin leaves in decibels per meter for vertical polarization is as follows:

$$\alpha^{(d)} = 91 f_{GHz} \chi_r'' \rho_d \pi \frac{t a_d^2}{\sin \theta_i} \times \left[1 - \left(\frac{1}{2} \cos^2(\theta_i) I_1^{(d)} + \sin^2(\theta_i) I_2^{(d)} \right) \right] \quad (8)$$

where

χ_r'' is the imaginary part of the relative susceptibility of a leaf,

f_{GHz} is the frequency (GHz),

ρ_d is the number density (m^{-3}),

t is the leaf thickness (m),

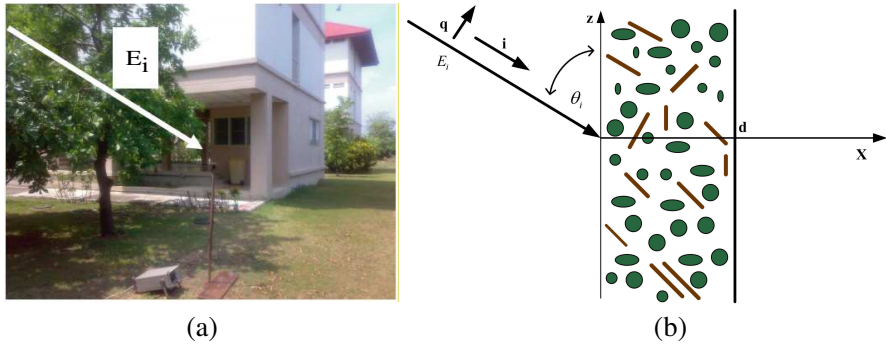(a)   (b)

Figure 5. Geometry of vegetation model: (a) Phenomena considered, (b) incident plane wave on the tree slab with thin leaves and thin branches.

a_d is the leaf radius (m), and

θ_i is the angle of incident plane wave as shown in Figure 5(b).

And

$$I_1^{(d)} = \int_{\theta_1^{(d)}}^{\theta_2^{(d)}} \sin^2(\theta) p^{(d)}(\theta) d\theta \tag{9}$$

$$I_2^{(d)} = \int_{\theta_1^{(d)}}^{\theta_2^{(d)}} \cos^2(\theta) p^{(d)}(\theta) d\theta \tag{10}$$

where $p^{(d)}(\theta)$ is the probability density of leaf inclination angle θ which is angle between the normal vector of a thin leaf and the Z-axis [11].

4. MEASUREMENT PROCEDURE AND SITES

The measurements were performed at frequencies of 900 and 1800 MHz. The equipments for propagation measurement consisted of a fixed CW transmitter and a portable spectrum analyzer. The transmitter consisted of HP 83732B signal generator (with 18 dBm output) and a quarter wave dipole antenna. We used HP 8593E spectrum analyzer with a 30 dB low noise amplify (LNA) and a quarter wave dipole antenna for signal strength measurement as shown in Figure 6. All measurements are co-vertical polarization.

We selected the dormitory for a measurement site. It consists of 3 main buildings with three story buildings, a two story building and 5 single story buildings for offices, a cafeteria and an auditorium in this area. The average height and % of buildings in the area are 9.5 m and 23% respectively. There are two marshes and vegetation in the area.

The transmitting antenna heights were fixed at 5.2 and 8.6 m above ground on the second and third floors of a dormitory building as shown by a rectangular dot in Figure 7, while the receiving antenna height is fixed at 1.6 m above ground. The receiver unit was moved
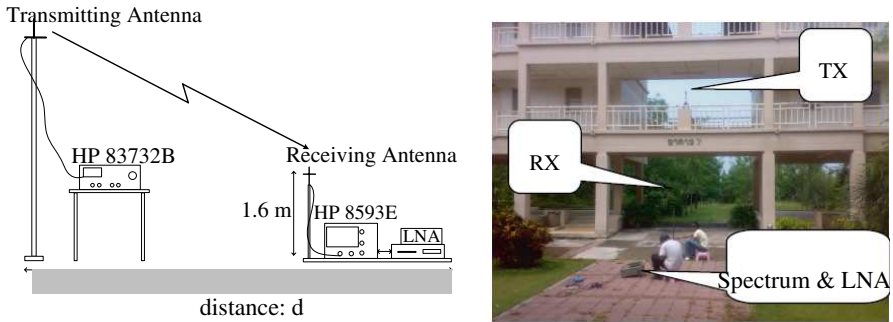

Figure 6. Measurement setup.

Figure 7. Measurement locations of the dormitory buildings.

to the measurement points as shown by circular dots in Figure 7. For each measurement point, at least 36 samples were taken over 40 wavelengths and averaged to the local average power. Therefore, the distance between two adjacent samples is 0.8λ in order to fulfill Lee's criteria [16].

The measurement was started on 30 March 2009 and completed on 29 April 2009. The equipment was calibrated before measurement by LOS measurement. Additionally, each measurement point was carried out twice in order to increase the reliability.

5. PREDICTION RESULTS

We modified the original model in (6) with airy building or tree model. The proposed model is then evaluated in term of its performance compared with the original building model. All prediction models are evaluated in terms of three performances measured, 1) Root Mean Square Error (RMSE) which measures the mean error deviation of measured path loss to predicted values of all measurement points, 2) Maximum Relative Error (MRE) which measures the largest error in predictions, finally 3) Correlation coefficient (R^2) as the index to show how good the regression is. Summaries of mathematic equations of these performance measures are as follows:

$$RMSE = \sqrt{\frac{\sum_{i=1}^{n}(m_i - \hat{m}_i)^2}{n}} \qquad (11)$$

$$MRE = \max\left(\frac{|m - \hat{m}|}{|m|}\right) \qquad (12)$$

$$R^2 = 1 - \frac{\sum_{i=1}^{n}(m_i - \hat{m}_i)^2}{\sum_{i=1}^{n}(m_i - \tilde{m}_i)^2} \qquad (13)$$

where m is the measured path loss array; n is the number of measurements; m_i is the measured path loss; $\hat{m}$ is the predicted path loss; $\tilde{m}_i$ is the mean of the measured path loss.

The objective of the comparison here is to present the effect of airy buildings and vegetation to path loss prediction on the image. The comparison between the proposed model which includes airy building or vegetation effects and the original model which excludes those effects, is comprised of three subjects. The first subject presents the overall average prediction error when the transmitting heights are 5.2 and 8.6 m, and frequencies are 900 and 1800 MHz. The performance measure RMSE is applied to indicate average path loss error at each

measurement point. The second comparison subject presents the average path loss error and the largest error in the prediction in two sub areas: (i) Wave propagation through airy buildings, and (ii) wave propagation through regular buildings and trees. The two performance measures RMSE and MRE are applied. The last subject presents the regression of measured path loss when the wave propagated through only the airy buildings.

Table 1. Summary of the building models parameters.

Point number	Path type	Environment category	Average building height (m) Tx = 8.6 m	Tx = 5.2 m	Mobile distance from transmitter (km)	Distance of mobile from the last rooftop (m)
1	Transverse	Airy Buildings	8	4.9	0.047	35
2	Transverse	Airy Buildings	8	4.9	0.056	47
3	Transverse	Airy Buildings	8	4.9	0.064	60
4	Transverse	Airy Buildings	8	4.9	0.066	71
5	Transverse	Airy Buildings	8	4.9	0.080	86
6	Transverse	Airy Buildings	8	4.9	0.082	96
7	Transverse	Airy Buildings	8	4.9	0.090	109
8	Transverse	Airy Buildings	8	4.9	0.103	122
9	Staircase	Regular Buildings, Trees	9.5	9.5	0.052	35
10	Staircase	Regular Buildings	9.5	9.5	0.072	4
11	Staircase	Regular Buildings, Trees	9.5	9.5	0.100	39
12	Lateral	Regular Buildings, Trees	9.5	9.5	0.072	5
13	Lateral	Regular Buildings, Trees	9.5	9.5	0.084	8
14	Lateral	Regular Buildings, Trees	9.5	9.5	0.094	9
15	Lateral	Regular Buildings, Trees	9.5	9.5	0.108	30
16	Staircase	Regular Buildings	9.5	9.5	0.058	1
17	Staircase	Regular Buildings	9.5	9.5	0.084	3

Table 2. Summary of the tree model parameters.

Point number	radius (cm)	Leaves thin (mm)	density (m^{-3})	Incident angle	Distance through tree (m)
9	4	0.5	180	70	4
11	3.5	0.5	250	80	8
12	5	0.2	960	45	6
13	8.5	0.2	240	45	11
14	4	0.2	320	45	8
15	5	0.2	160	70	12

Table 3. Comparison of the models at measurement points for all transmitter locations and frequencies.

Measurement Point Number	Distance (m)	Building	Road	Tree	Plain	Water	RMSE Original model	RMSE Proposed model
1	47	8	39	0	0	0	12.83	2.16
2	56	8	48	0	0	0	12.46	2.49
3	64	8	56	0	0	0	11.25	1.69
4	66	8	58	0	0	0	9.95	3.12
5	80	8	72	0	0	0	12.02	2.46
6	82	8	74	0	0	0	10.90	3.05
7	90	8	82	0	0	0	12.59	1.81
8	103	8	95	0	0	0	15.25	2.73
9	52	5	20	6	8	14	5.38	4.17
10	72	16	7	0	30	19	3.56	3.56
11	100	1	43	8	25	22	9.47	5.08
12	72	27	9	6	30	0	7.47	4.44
13	84	17	4	11	51	0	9.94	5.12
14	94	50	6	8	30	0	7.56	5.22
15	108	42	8	12	46	0	11.00	5.28
16	58	26	6	0	27	0	3.33	3.33
17	84	35	13	0	37	0	3.32	3.32
						Average	9.31	3.47

Summaries of the parameters of building and tree models are shown in Tables 1 and 2 respectively. Note that the building heights of transverse path loss in Table 1 are lower than the transmitting antenna heights because of the airy building model in Figure 4. The results of the first comparison subject are given in Table 3. We found that the proposed model provides better accuracy than the original model in (6) at the measurement points 1 to 8 because of the airy building effects. While the proposed model, which comprises of the original model and vegetation effect, generally provides better accuracy than the original model at measurement points 9 and 11 to 15 because of vegetation effects. The path loss errors between the original model and the proposed model are equal since there are no effects from the airy building and vegetation at measurement points 10, 16 and 17.

Tables 4 and 5 show the results of the second comparison subject. From both tables we found that the RMSE values of the proposed model are generally lower than the original one. The RMSE of the

Table 4. Comparison of the models at frequency of 900 MHz.

Model	RMSE	MRE
Tx 5.2 m		
Meas. No. 1–8		
Original	13.5505	0.4276
Proposed	4.1511	0.3065
Meas. No. 9–17		
Original	8.9850	0.1641
Proposed	4.0546	0.1181
Tx 8.6 m		
Meas. No. 1–8		
Original	7.8108	0.1950
Proposed	3.5104	0.2047
Meas. No. 9–17		
Original	11.2021	0.2585
Proposed	5.6344	0.1261

Table 5. Comparison of the models at frequency of 1800 MHz.

Model	RMSE	MRE
Tx 5.2 m		
Meas. No. 1–8		
Original	16.8179	0.3297
Proposed	2.6812	0.1373
Meas. No. 9–17		
Original	7.4882	0.1842
Proposed	5.7926	0.1505
Tx 8.6 m		
Meas. No. 1–8		
Original	13.1381	0.3662
Proposed	1.9858	0.1016
Meas. No. 9–17		
Original	6.0740	0.1721
Proposed	4.0649	0.1240

measurement points 1 to 8 occur from the airy building effects. While those values of the measurement points 9 to 17 occur from the regular building with or without tree losses. The MRE values of the proposed model are generally lower than the original model as shown in the

tables. These values depend on time-varying effect from people moving in the building and/or on the road. The comparison among measured, original, and proposed models at the transmitting heights of 5.6 and 8.6 m for frequencies of 900 and 1800 MHz is shown in Figures 8 and 9
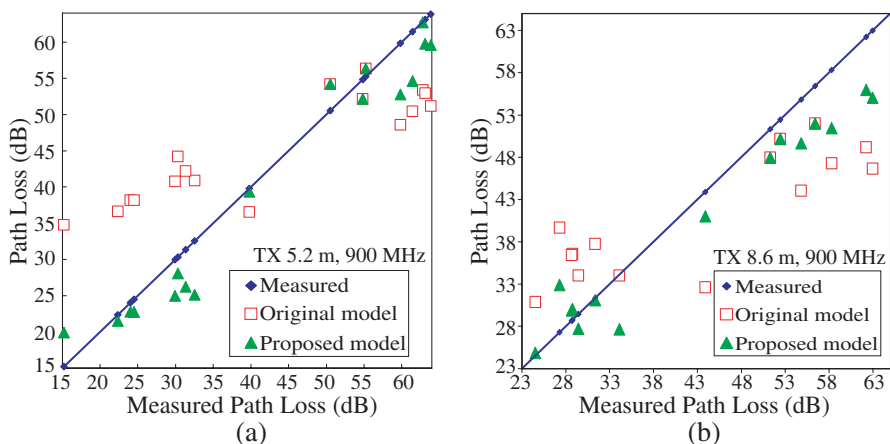

Figure 8. Comparison between measured original and proposed models at frequency of 900 MHz at transmitting antenna height of (a) 5.2 m and (b) 8.6 m.
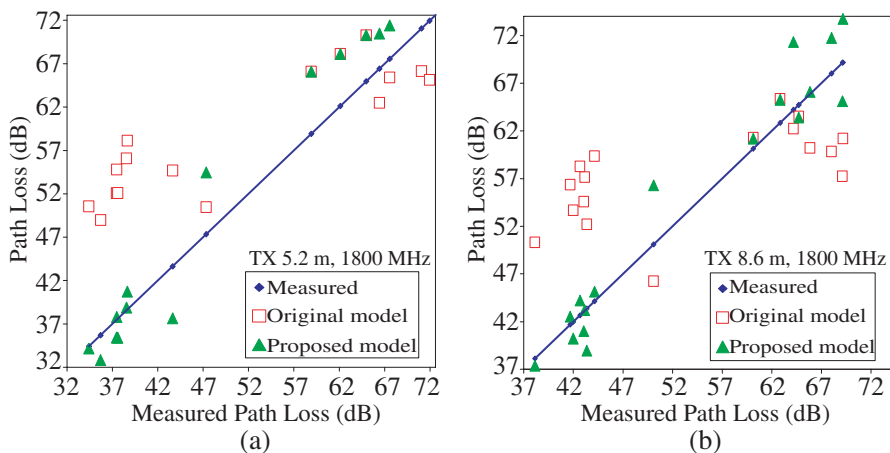

Figure 9. Comparison between measured original and proposed models at frequency of 1800 MHz at transmitting antenna height of (a) 5.2 m and (b) 8.6 m.

respectively. The oblique lines in the figures represent the measured path loss values of their measurement points. It can be seen that the predicted path losses from the proposed model (triangle dots) provide good agreement with the original model (rectangular dots).

The linear fit of measured path loss in transverse locations at measurement points 1 to 8 is shown in Figure 10. From the regression lines of the measured signals and their R^2, it is found that the signal strength at the transmitting antenna height of 5.2 m and frequency of 900 MHz tends to rapid decrease as shown with the blue regression line in Figure 10. This is because of the first Fresnel zone region. The breakpoint distance d_{bp}, for the wavelength λ, can be calculated by $4h_b h_m/\lambda = 100$ m which is in the range of the measurement point. This makes the signal strengths at distance after breakpoint become low quickly. The diameter of the first Fresnel zone region is $Z_f \approx \sqrt{\lambda d_{bp}}$ or 5.8 m. This zone is mostly interfered by obstructions. Therefore the signal propagates in case of NLOS rapidly attenuated. The R^2 of 0.771 confirms this phenomenon. While the other regression lines in Figure 10 provide low slopes since their d_{bp} are in the range of 165–
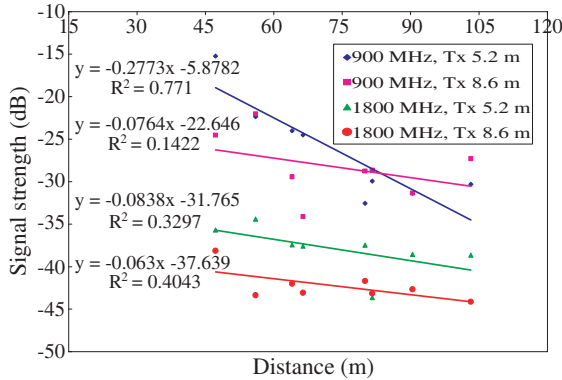

Figure 10. Regression of measured signal at transverse measurement points.

Table 6. Break point distance and diameter of first Fresnel zone.

Frequency	Break point distance (m)		Diameter of first Fresnel zone (m)	
(MHz)	Tx=5.2 m	Tx=8.6 m	Tx=5.2 m	Tx=8.6 m
900	100	165	5.8	7.4
1800	200	330	5.8	7.4

330 m from the transmitter which are far from the measurement points and the diameters of the first zone which are in the range of 5.8–7.4 m. This make the zones t free from obstructions. Therefore, the waves can propagate via the zones to the receiving antenna with low attenuation. Summaries of the break point distances and the diameters of the zone are shown in Table 6.

6. CONCLUSION

We have proposed a radio wave propagation prediction method with 2-D aerial images using image classification. The images were classified by the CTP_MLA to identify the objects in the interesting areas. The segmented objects consist of roads, trees, buildings, plains and water which have a high influence on wave propagation. Hence, the path losses were predicted on the classified image using modified Xia model. We have modified the original Xia model with including the effects of airy buildings and vegetation. To verify the proposed model, the measurements were performed in realistic areas at two frequencies, 900 MHz and 1800 MHz. From the results it is found that the proposed model provides good agreement, especially in the case of the airy buildings.

ACKNOWLEDGMENT

REFERENCES

1. Xia, H. H., "A simplified model for prediction path loss in urban and suburban environments," *IEEE Trans. Veh. Technol.*, Vol. 46, No. 4, 1040–1046, Nov. 1997.

2. Har, D., H. H. Xia, and H. L. Bertoni, "Path-loss prediction model for microcells," *IEEE Trans. Veh. Technol.*, Vol. 48, No. 5, 1453–1462, Sep. 1999.

3. Walfisch, J. and H. L. Bertoni, "A theoretical model of UHF propagation in urban environments," *IEEE Trans. Ant. Prop.*, Vol. 36, No. 12, 1788–1796, 1988.

4. Ikegami, F., S. Yoshida, T. Takeuchi, and M. Umehira, "Propagation factors controlling mean field strength on urban streets," *IEEE Trans. Ant. Prop.*, Vol. 32, 822–829, 1984.

5. Oda, Y., K. Tsunekawa, and M. Hata, "Advanced LOS path loss model in microwave mobile communications," *IEEE Trans. Veh. Technol.*, Vol. 49, 2121–2125, Nov. 2000.

6. Jiang, L. and S. Y. Tan, "A simple analytical path loss model for urban cellular communication systems," *Journal of Electromagnetic Waves and Applications*, Vol. 18, No. 8, 1017–1032, 2004.

7. Masui, H., T. Kobayashi, and M. Akaike, "Microwave path loss modeling in urban line-of-sight. Environments," *IEEE J. Select. Areas Commun.*, Vol. 20, No. 6, 1151–1155, Aug. 2002.

8. Durgin, G., T. S. Rappaport, and H. Xu, "Measurements and models for radio path loss and penetration loss in and around homes and trees at 5.85 GHz," *IEEE Trans. on Commun.*, Vol. 46, No. 11, 1484–1485, Nov. 1998.

9. Karlsson, A., R. E. Schuh, C. Bergljung, P. Karlsson, and N. Löwendahl, "The influence of trees on radio channels at frequencies of 3 and 5 GHz," *VTC 2001 Fall. IEEE VTS 54th*, Vol. 4, 2008–2012, Oct. 2001.

10. Torrico, S. A., H. L. Bertoni, and R. H. Lang, "Modeling tree effects on path loss in a residential environment," *IEEE Trans. Ant. Prop.*, Vol. 46, No. 6, 872–880, Jun. 1998.

11. Torrico, S. A. and R. H. Lang, "A simplified analytical model to predict the specific attenuation of a tree canopy," *IEEE Trans. Veh. Technol.*, Vol. 56, No. 2, 696–703, Mar. 2007.

12. Meng, Y. S., Y. H. Lee, and B. C. Ng, "Measurement and characterization of a tropical foliage channel in VHF and UHF bands," *10th IEEE Singapore Inter. Conf. (ICCS 2006)*, 1–5, Oct. 2006.

13. Kürner, T. and A. Meier, "Prediction of outdoor-to-indoor coverage in urban areas at 1.8 GHz," *IEEE J. on Selected Areas in Commun.*, Vol. 20, No. 3, 496–506, April. 2002.

14. Teeranachaideekul, N., P. Phokharatkul, S. Ongwattanakul, B. Emaruchi, and S. Phaiboon, "A maximum likelihood method for the classification of aerial photographs," *Proc. JCSSE2007*, 254–259, May 2–4, 2007.

15. Perkins, T. C., "Remote sensing image classification and fusion for terrain reconstruction," B.S.E.E., University of Louisville, 1999.

16. Lee, W. C. Y., "Estimate of local average power of a mobile radio signal," *IEEE Trans. Veh. Technol.*, Vol. 34, No. 1, 22–27, Feb. 1985.